Video Article

Use of Ultra-high Field MRI in Small Rodent Models of Polycystic Kidney Disease for *In Vivo* Phenotyping and Drug Monitoring

Maria V. Irazabal[1], Prasanna K. Mishra[2], Vicente E. Torres[1], Slobodan I. Macura[2]

[1]Department of Internal Medicine, Division of Nephrology, Mayo Clinic

[2]Department of Biochemistry and Molecular Biology, Mayo Clinic

Correspondence to: Maria V. Irazabal at irazabalmira.maria@mayo.edu

Abstract

Several *in vivo* pre-clinical studies in Polycystic Kidney Disease (PKD) utilize orthologous rodent models to identify and study the genetic and molecular mechanisms responsible for the disease, and are very convenient for rapid drug screening and testing of promising therapies. A limiting factor in these studies is often the lack of efficient non-invasive methods for sequentially analyzing the anatomical and functional changes in the kidney. Magnetic resonance imaging (MRI) is the current gold standard imaging technique to follow autosomal dominant polycystic kidney disease (ADPKD) patients, providing excellent soft tissue contrast and anatomic detail and allowing Total Kidney Volume (TKV) measurements.A major advantage of MRI in rodent models of PKD is the possibility for *in vivo* imaging allowing for longitudinal studies that use the same animal and therefore reducing the total number of animals required. In this manuscript, we will focus on using Ultra-high field (UHF) MRI to non-invasively acquire *in vivo* images of rodent models for PKD. The main goal of this work is to introduce the use of MRI as a tool for *in vivo* phenotypical characterization and drug monitoring in rodent models for PKD.

Video Link

The video component of this article can be found at http://www.jove.com/video/52757/

Introduction

Polycystic Kidney Disease (PKD) includes a group of monogenic disorders characterized by the development of renal cysts. Among them are autosomal-dominant polycystic kidney disease (ADPKD) and autosomal-recessive polycystic kidney disease (ARPKD), which represent the most common types[1,2]. ADPKD, the most frequent form of hereditary renal cystic diseases, is originated by mutations in the *PKD1* or *PKD2* genes. It is characterized by late-onset, multiple bilateral renal cysts, accompanied by variable extra-renal cysts, as well as cardiovascular and muscle skeletal abnormalities. ARPKD, most commonly affecting newborns and young children, is caused by mutations in *PKHD1* and is characterized by enlarged echogenic kidneys and congenital hepatic fibrosis[3].

Importantly, ADPKD is characterized by heterogeneity, both at the gene (genic) and mutation (allelic) levels, which results in substantial phenotypic variability. Mutations in the *PKD1* gene are associated with severe clinical presentation (numerous cysts, early diagnosis, hypertension, and hematuria), as well as rapid progression to end-stage renal disease (20 years earlier than patients with *PKD2* mutations)[4]. Severe polycystic liver disease (PLD) and vascular abnormalities can be associated with mutations in both *PKD1* and *PKD2*[5]. The majority of renal complications of ADPKD arise mainly as a consequence of the cyst expansion along with associated inflammation and fibrosis. Cyst development starts *in utero* and continues through the patient lifetime. Kidneys usually maintain their reniform shape even though they could reach more than 20 times the normal kidney volume. Most of the patients present bilateral distribution of renal cysts, but in some unusual cases, cyst may develop in a unilateral or asymmetric pattern.

A major challenge for nephrologists following patients with ADPKD or implementing therapies is the natural history of the disease. During most of its course, the renal function remains normal and by the time the renal function starts to decline, most of the kidneys have been replaced by cysts. When therapies are implemented at later stages, it is less likely to be successful since the patient may already have reached a point of no return in chronic kidney disease. In contrast, when therapies are started at early stages, it is difficult to identify a response based solely on glomerular filtration rate. As a result, the notion of kidney volume as a marker of disease progression gained attention.

The Consortium for Radiologic Imaging Studies of Polycystic Kidney Disease (CRISP) study has shown that in patients with ADPKD the increase in kidney and cyst volumes directly correlates with renal function deterioration, underscoring the potential of Total Kidney Volume (TKV) as a surrogate marker for disease progression[6,7]. Consequently, TKV is currently used as primary or secondary endpoint in multiple clinical trials for ADPKD[2,8,9].

Multiple murine models including spontaneous mutations and genetically engineered have shed light on the pathogenesis of PKD[10,11]. Pkd1 or Pkd2 models (mutations in either *Pkd1* or *Pkd2*) have become the most popular ones, as they perfectly mimic human disease. In addition, rodent models with mutations in genes other than *Pkd1* or *Pkd2* genes have been used as an experimental platform to elucidate signaling pathways related to the disease. In addition, several of these models have been used to test potential therapies. However, a limiting factor in many rodent studies for PKD is often the lack of efficient non-invasive methods to sequentially analyze the anatomical and functional changes in the kidney.

Magnetic resonance imaging (MRI) is the current gold standard imaging technique to follow ADPKD patients, providing excellent soft tissue contrast and anatomic detail, and allowing TKV measurements. Even though MRI is well established for anatomical imaging in larger animals and humans, imaging small rodents *in vivo* entails additional technical challenges, where the ability to acquire high resolution images may limit its usefulness. With the introduction of Ultra-high field (UHF) MRI (7-16.4 T) and the development of stronger gradients, it is now possible to achieve higher signal-to noise ratios and spatial resolution of MRI images with a diagnostic quality similar to that obtained in humans. Consequently, the use of UHF MRI for *in vivo* imaging of small rodent models for PKD has become a powerful tool for researchers.

Protocol

Before starting any procedures with live animals, experimental protocols should be approved by the institutional animal care and use committee (IACUC).

1. Scanner Configuration

1. Before starting, make sure the heater is in OFF position.
2. Select the mini imaging gradient and 38 mm RF coil and mini imaging holder.
3. In the central bore of the holder install the variable temperature assembly.

2. Animal Preparation

1. For MRI experiments, achieve optimal anesthesia using vaporized isoflurane. For induction of anesthesia, place animal in an induction chamber lined with an absorbent tissue. Adjust the flowmeter of the isoflurane vaporizer to 2.0-2.5 L/min, and the isoflurane to 3% in oxygen.
2. Remove any metal tag or other metallic object at this stage. Apply vet ointment on animal's eyes to prevent dryness while under anesthesia.
3. Once the animal has reached the surgical plane of anesthesia (*i.e.,* loss of withdrawal reflex to toe pinch), place the animal on a holder with its nose inserted into a nose cone. Set the anesthesia air flow in the probe to 2.0-2.5 ml/min and the isoflurane concentration to 1.5-2.0% in oxygen. Anesthesia will be delivered through the nose cone during the procedure. Periodically adjust isoflurane concentration depending on animal's age and weight to maintain a respiration rate of ~40 bpm.
4. Use animal holders to secure the animal in place and prevent motion during the MRI experiment. Vary the type of animal holder depending on the body region to be scanned.
   Note: Customized holders from laboratory plastics (polypropylene, Teflon, polystyrene, polycarbonate) can be made to accommodate specific experiment and to fit the animal size (from newborn mouse to 160 g rat).
5. Place the rectal thermometer in the animal to monitor animal's body temperature. During the experiment, keep the animal at 35-37 °C, using a stream of warm air. Adjust air temperature (30-38 °C) and flow (1,200-2,000 L/hr) based on animal's body temperature feedback.
6. Attach a balloon respiratory pressure sensor to animal's abdomen to monitor respiration rate.
7. Secure the animal at the center of the RF coil and carefully place the RF coil with animal into MRI scanner.

3. MRI Experiment

1. Tune and match the RF coil before starting the experiments to minimize RF power used and to maximize signal-to-noise ratio. To start the matching/tuning:
   1. Open the spectrometer control tool by clicking the tools icon.
   2. In the spectrometer control tool click Acquisition → Wobble. An Acq/Reco window will open displaying the wobble curve.
   3. Alternatively adjust the tuning and matching capacitors (using the tuning and matching rods) in small steps until the reflected RF power is minimized. The goal is to see a curve with a minimum at the vertical axis positioned at zero on the horizontal axis.
   4. When the calibration of the coil has been successfully achieved, hit the Stop button in the Acq/Reco window.

2. Acquire scout images in the three orthogonal planes to create axial, coronal and sagittal images. Use a fast image sequence such as Intra Gate Fast Low Angle Shot (IG-FLASH) to acquire the scout images[12]. Use the scout images to set the proper geometry for the actual imaging.
3. Depending on the specific research aims, select proper image sequence and parameters and start the scan with a traffic light. This will calibrate RF channel, shim the magnet, set carrier frequency on-resonance for water and adjust receiver gain, all automatically.
   1. For anatomic studies and T2 weighted images, acquire in 2D multi slice or 3D mode. To shorten the experiment time for a given spatial resolution, keep the field-of-view (FOV) as small as possible but large enough to avoid wrap-around artifacts (2.56-3.2 cm).

4. Keep the cycle of selected sequence slightly shorter than the animal respiration cycle by proper selection of repetition time (TR) and/or number of slices. This ensures that the data are collected during animals' quiet period.
   1. For example, for abdominal images, keep animal's respiratory rate at ~30 bpm; that is about 2,000 msec per breath. Use a Turbo Rapid Acquisition with Relaxation Enhancement (RARE) sequence and acquire 11-19 coronal slices, with TR/TE 1500/9 msec, RARE factor 8 and (matrix 256 x 256, FOV 2.56 x 2.56 cm, slice thickness 0.75 mm).
   Note: By adjusting the TR to 1,500 msec, and keeping the animal's respiratory rate ~30 bpm (2,000 msec per breath), we ensure that the data are collected during animals' quiet period.

5. After all image acquisition has been completed, place the scanned animal on heated pad and monitor until ambulatory. After recovery, return the animal to the cage and monitored at least for 1 hr before returning to the animal facility.

Representative Results

In this manuscript, we aim to show the usefulness of UHF MRI as a tool for *in vivo* phenotypical characterization or drug monitoring in rodent models for PKD and other kidney diseases. All of the experiments were part of experimental protocols approved by the IACUC.

In vivo phenotyping of small rodent models for PKD using UHF MRI:

All imaging studies were performed on live animals under isoflurane anesthesia, with a Bruker AVANCEIII-700 (16.4 T) vertical-bore two channel multinuclear spectrometer, equipped with mini and micro-imaging accessories for *in vivo* and *in vitro* NMR spectroscopy and microscopy.

Abdomen:

The main structural change in PKD is cyst development and growth that are responsible for the majority of renal complications. The most common extra-renal manifestation in ADPKD is the presence of hepatic cysts and can be found in up to 90% of affected adults[13]. Using UHF MRI, it is possible to acquire high definition, anatomical abdominal images of small PKD rodents that allow for *in vivo* assessment of the cystic phenotype and kidney volume measurements. **Figure 1A-D** shows multiple 2D T2 weighted anatomical abdominal images for different rodent models of PKD. Abdominal images were acquired using a 38 mm volume RF coil. An MRI compatible holder was used to place animals vertically along the magnetic field. A balloon sensor was used to monitor respiration. Respiratory gating was performed. Then, coronal, sagittal, and axial, scout images were acquired in order to locate the kidneys and prescribe its geometry. A turbo Rapid Acquisition with Relaxation Enhancement (RARE) sequence, 11-19 coronal slices with TR/TE 1,500/9 msec, RARE factor 8, (matrix 256 x 256, FOV 2.56 x 2.56 cm, slice thickness 0.75 mm) was used to collect anatomical images.

Heart:

Cardiovascular complications remain an important problem in patients with ADPKD, associated with increased morbidity and mortality[14,15]. Experimental and clinical MRI allows accurate and reproducible assessment of cardiac structure and function[16-18]. MRI possesses high temporal and spatial resolution, allowing optimal visualization and analysis of the small-sized, fast-beating rodent heart. For this reason, it is feasible to use UHF MRI to acquire cardiac images to calculate end-diastolic volume (EDV), end-systolic volume (ESV) as well as myocardial mass from sequential short axis cines covering the entire heart in several rodent models of PKD. **Figure 2** shows MRI images of the mouse myocardium. Cardiac cine images are acquired using Intra Gate-Fast Low-Angle Shot (ig-FLASH) sequence[19] (11 short axis slices, TR/TE 3.5/1.45 msec, repetition 100, matrix 256 x 256, FOV 2.56 x 2.56 cm, slice thickness 1 mm).

Brain:

Many ciliopathies have been associated with brain malformations among other defects. Over the past years, MRI has become the gold-standard for non-invasive imaging of the brain. Unlike histological studies, MRI offers detection of anatomical changes without preparation artifacts that interfere with normal examination. We use UHF MRI to assess the brain phenotype of multiple mice models for PKD, or other modifier genes related to the disease. **Figure 3** shows anatomical images of the mouse brain. Images were acquired using a turbo RARE sequence, 11-13 axial slices and 25-29 coronal slices with TR/TE 1,500/9 msec, RARE factor 8, (matrix 256 x 256, FOV 2.56 x 2.56 cm, slice thickness 0.75 mm).

In vivo MRI of mouse embryos inside the maternal uterus:

The possibility of gathering *in vivo* information about embryo number, viability, developmental stage, as well as assess phenotypic differences of the embryos, is of importance especially when exploring the effect of inactivating specific signaling pathways in combination with *Pkd1* or *Pkd2* specific mutations. By performing *in vivo* MRI of pregnant females, it is possible to detect embryonic lethality and assess for phenotypic abnormalities, and when present, determine at what embryonic stage they occurred. **Figure 4** shows an example that detailed embryonic information can be obtained from pregnant females using *in vivo* UHF MRI. Abdominal images were acquired as previously described for non-pregnant animals. Isoflurane may be safely used in pregnant rodents and anesthesia is achieved as in non-pregnant animals[20]. By embryonic day 13 (E13), it is possible to identify many anatomical features such as the limb buds, midbrain, telencephalon and heart. From E14-15 the metanephros can be pointed out, appearing as an ovoid structure (1-1.5 mm in length) with a medullary and a cortical component[21].

In vivo disease progression or treatment monitoring of small rodent models for PKD using UHF MRI:

In addition to providing excellent anatomic detail, UHF MRI allows for TKV measurements in rodent models for PKD. As in patients, TKV can be used to monitor disease progression or assess drug interventions before a change in renal function can be perceived. Furthermore, the possibility of imaging neonatal rodents provides an important entry point for MRI studies in which *in utero* interventions are performed. **Figure 5** shows multiple 2D T2 weighted anatomical abdominal images for a PCK rat study that used TKV as end-point. Abdominal images were acquired as previously described.
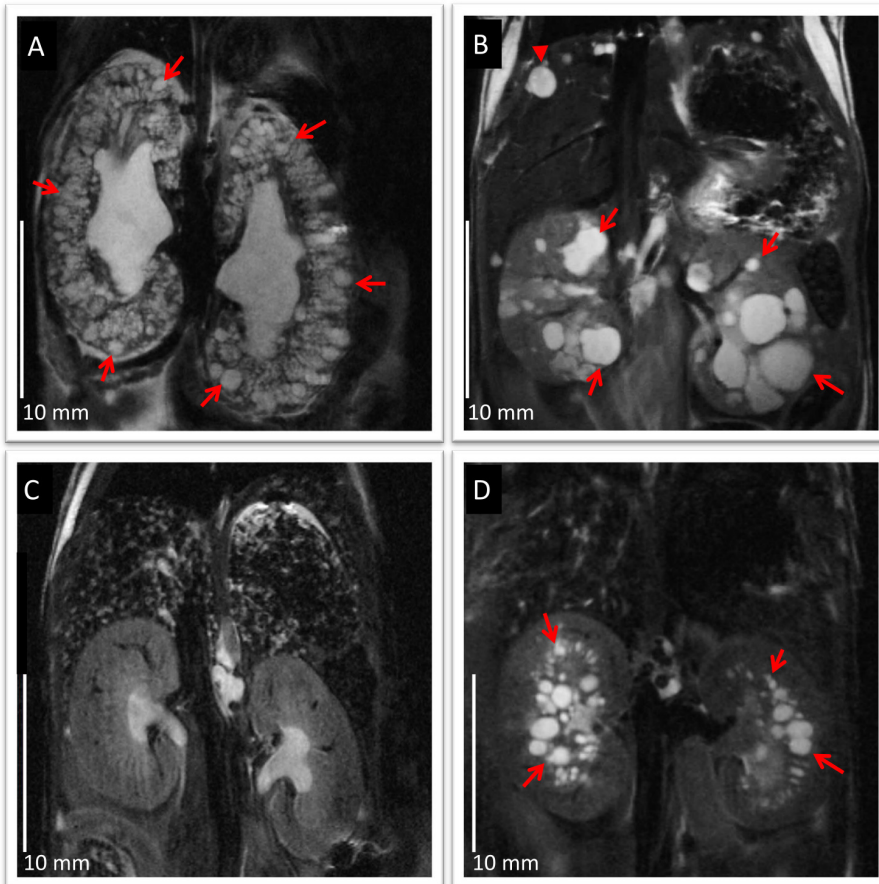
Figure 1: Anatomical coronal abdominal MRI images for different rodent models of PKD. (**A**) 19 month old *Pkd1*[RC/RC] mouse showing almost complete replacement of kidney tissue by cysts (arrows), mimicking typical changes in ADPKD, (**B**) 4 month old *Pkd2*[-/ws25] mouse showing bilateral renal cysts (arrows) and remaining renal parenchyma, and hepatic cysts (arrow heads), (**C**) 4 month old *Pkhd1*[lsl/lsl] mouse showing liver fibrosis and no kidney cysts, and (**D**) 21 days old PCK rat showing multiple bilateral renal cysts (arrows) predominantly at the corticomedullary region and outer medulla, and mild bile duct dilation. Images show good anatomical detail for phenotypic characterization, with in-plane resolution of 100 μm/pixel and slice thickness 750 μm. Note the difference between polycystic kidneys (**A**, **B** and **D**) compared to normal appearing kidneys (**C**). Scale bars: 10 mm. Please click here to view a larger version of this figure.
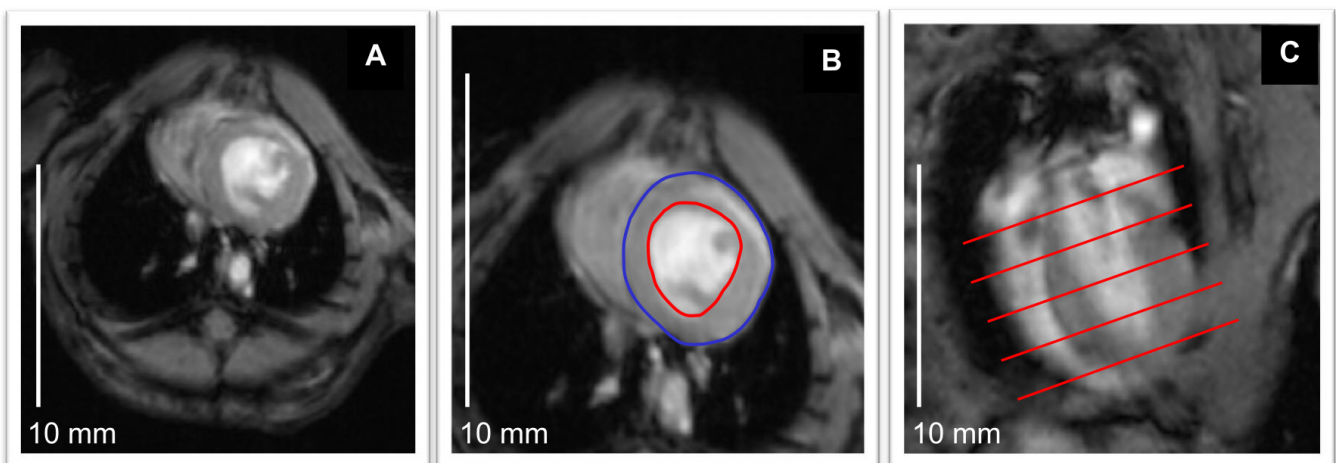

Figure 2: Cardiac morphology and function. (**A**) Anatomical image of the mouse heart from short axis, ig-FLASH sequence. (**B**) Outlining of endocardial border at end-diastole (red) allows calculating end-diastolic volume (EDV) for each slice. The same procedure can be done for end-systolic volume (ESV). In addition, myocardial volume (red-blue) can be calculated for each slice from short axis, cine images[22]. (**C**) Long axis image shows that overall EDV and ESV can be obtained by adding each slice's volume, and further calculate stroke volume and ejection fraction. Scale bars: 10 mm. Please click here to view a larger version of this figure.
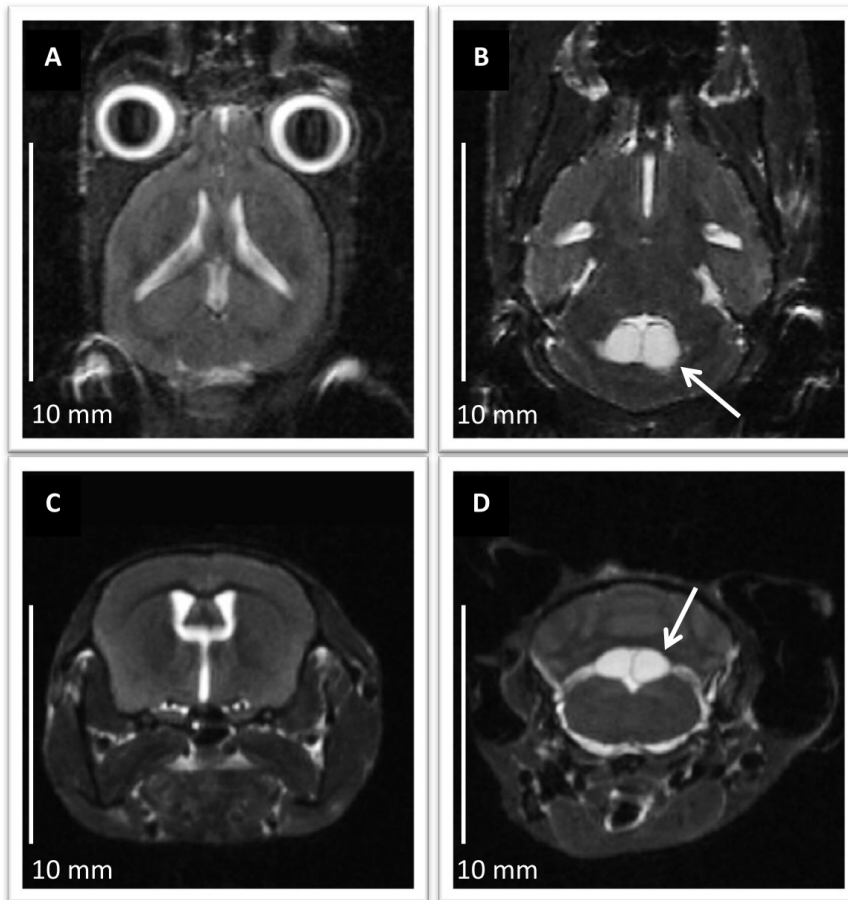
Figure 3: Anatomical imaging of mouse brain with UHF MRI. (**A**) and (**B**) axial, (**C**) and (**D**) coronal images of the brain in an ADPKD mouse model, acquired in 2D T2 weighted turbo-RARE sequence. The image in-plane resolution of 100 μm/pixel and slice thickness 750 μm allows for analyzing gross brain anatomy. In (**B**) and (**D**) the white arrows point to arachnoid cysts found in the area of the fourth ventricle. Scale bars: 10 mm. Please click here to view a larger version of this figure.
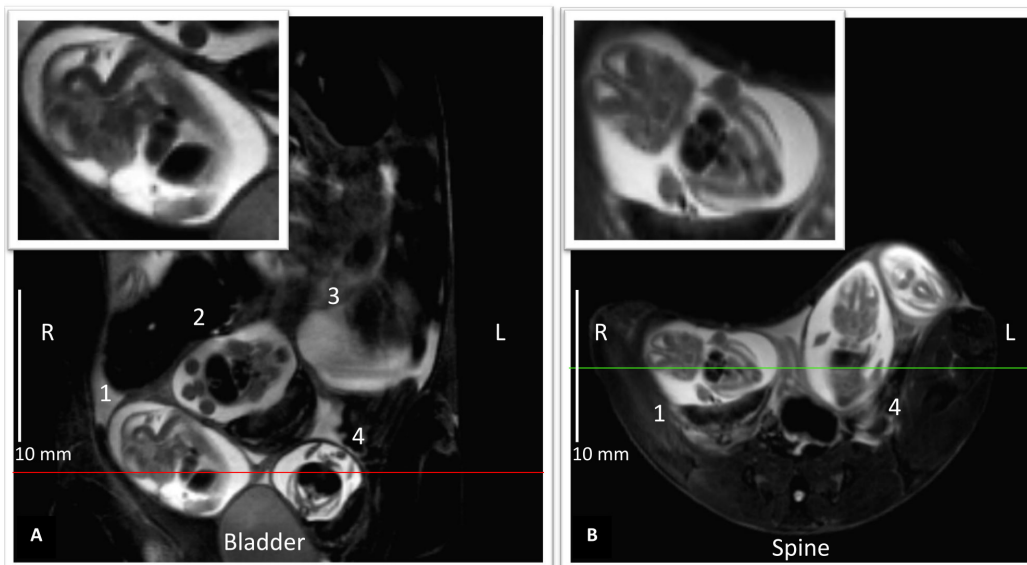

Figure 4: *In utero* imaging of E14 mouse embryos. T2 weighted turbo-RARE images acquired in the maternal coronal plane (**A**) and (**B**) maternal axial plane. **A** shows 4 different embryos 1-4 and **B** embryo 1 and 4, and an additional embryo not seen in **A**. Upper insets, magnified images from embryo 1, display embryo's sagittal plane **A,** positioned with the head pointing upward-right, its back to the left, and embryo's coronal plane **B**. The image in-plane resolution of a 100 μm/pixel allows identification of many anatomical features such as the limb buds, midbrain, telencephalon, heart and liver. Image scale bars: 10 mm. Please click here to view a larger version of this figure.
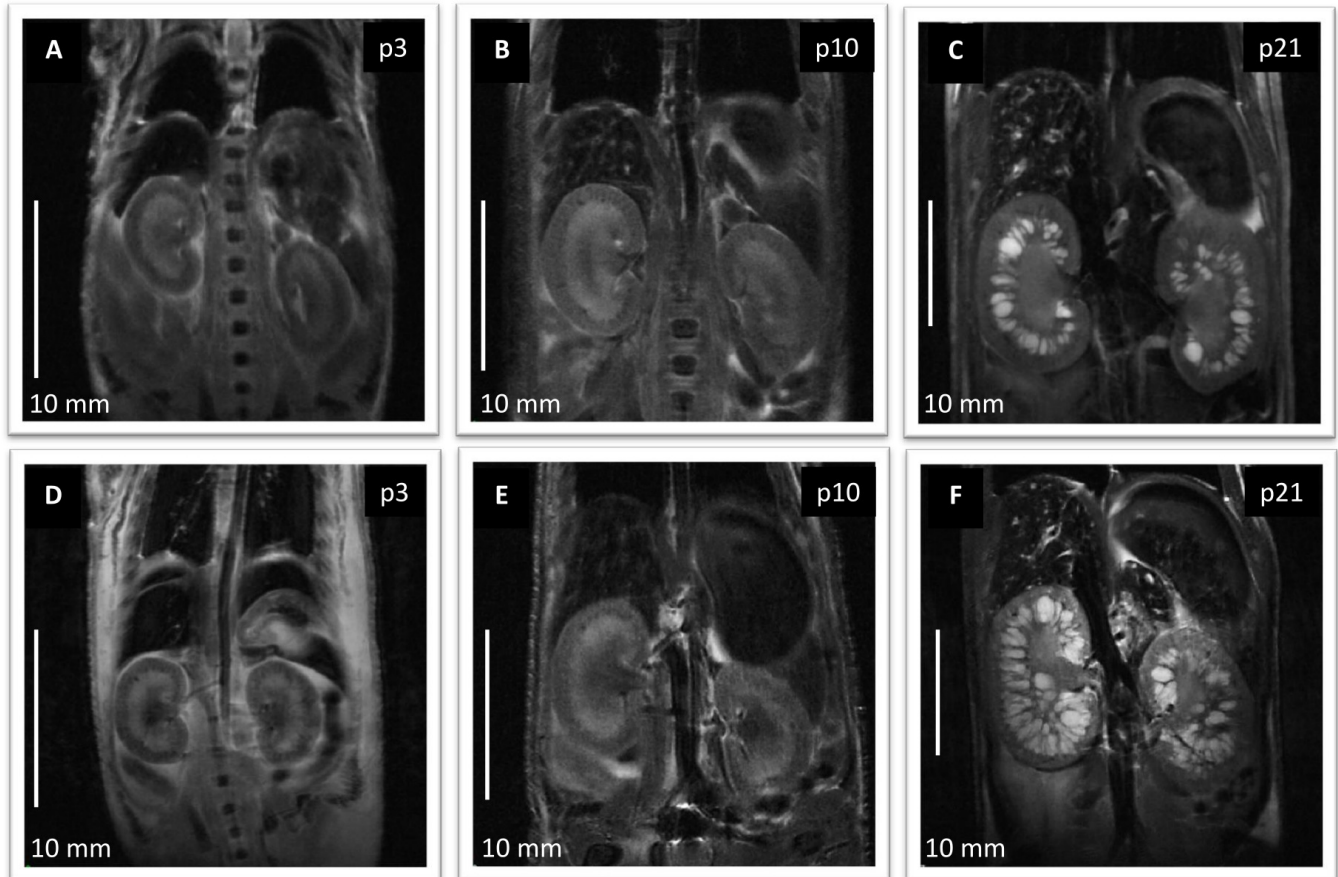
Figure 5: Anatomical coronal abdominal MRI images in a PCK rat study. (**A**-**C**) represent the control group (saline treated). Images were acquired from the same animal at p3, p10 and p21. (**D**-**F**) represent the treatment group (1-deamino-8-d-arginine vasopressin treated). Images were acquired from the same animal at the same ages as the control. Scale bars: 10 mm. Please click here to view a larger version of this figure.

Discussion

This manuscript shows the feasibility of using UHF MRI as a tool for *in vivo* phenotypical characterization or drug monitoring in rodent models for PKD.

We describe experiments done at 16.4 T with a wide bore Avance III high resolution NMR spectrometer equipped with micro and mini imaging accessories. The spectrometer was driven by the acquisition and processing software TopSpin2.0PV controlled by Paravision 5.1 imaging software. Because the rodent size varies in longitudinal studies, we used the mini imaging accessories with 38 mm RF coil and mini imaging holder. For the animal temperature control we used standard high resolution **v**ariable **t**emperature **u**nit (VTU BVT 3000 digital) guided by TopSpin 2.0. The airstream fed from the bottom of the probe passes over the heater and then by the thermocouple which is positioned immediately below the anesthetized rodent. The thermocouple controls the power level of the heater continuously changing it, to keep the air temperature at desired setting.

One of the main advantages of using UHF MRI for phenotypic characterization of rodent models of PKD is the possibility for acquiring *in vivo* images, thus allowing for longitudinal studies performed in the same animal. Advantages of longitudinal studies include decreased costs of husbandry and data variability, as well as analysis of phenotype progression or regression in models with incomplete penetrance.Another benefit of MRI vs conventional histology is that MR images present a more realistic anatomy without the shrinkage and distortion inherent in histological sections. Furthermore, MRI allows for 3D reconstruction of the images.

In addition to providing excellent anatomic detail, MRI allows for *in vivo* TKV measurements. TKV can be used to monitor disease progression over time, and asses drug interventions before a change in renal function occurs. Moreover, the possibility of imaging neonatal rodents provides an important entry point for studies in which *in utero* interventions are performed.

Despite its great advantages, *in vivo* imaging of rodent models for PKD is still challenging. This is especially true for mice and neonatal rats due to their small size and higher respiratory and heart rates compared to humans. The use of UHF MRI and stronger gradients allows for higher signal-to-noise ratios and better spatially resolved images, yet MRI is highly sensitive to motion, and motion artifacts can significantly decrease image resolution, reducing the benefits from the technique. This is particularly important for abdominal imaging which is of major interest in PKD. Breath hold scans, as acquired in humans, are not feasible without the insertion of an endotracheal tube (ET). The possibility of controlling an anesthetized animal's airway with an ET is advantageous in the event of cardiac or respiratory arrest; however, intubation of a rodent requires high technical skills and is difficult to master. Delivery of inhalant anesthesia such as isoflurane by face-mask is easy and is

the option of choice for most MRI procedures[23]. However, the possibility of hypoxia/asphyxia must be considered if the animal is not properly positioned while under anesthesia, and there is no control of the airway in the event of an emergency. Thus, careful monitoring of the animal's breathing rate and respiratory targeted sequences become highly important. In addition, achieving optimal anesthesia and animal positioning is essential for acquiring high resolution images on a scanner. As for all live animal studies, especially when using disease, neonatal or aged animals, it is critical to monitor the animal's vital parameters and maintain a stable physiological state during the procedure, to ensure animal health and the long term success.

In spite of its challenges, considerable progress has been made with UHF MRI allowing for detailed phenotypic information in small rodent models of PKD and becoming a powerful tool for *in vivo* phenotyping and drug monitoring. *In utero* images of developing embryos allow for early characterization of the phenotype associated with a genetic mutation and can identify cases of non-viable embryos. *In vivo* MRI is critical to achieve maximal benefit from rodent models of PKD (or any other rodent model system) and should be considered in any experimental design.

Disclosures

The authors have nothing to disclose.

Acknowledgements

References

1. Torres, V. E., Harris, P. C. Autosomal dominant polycystic kidney disease: the last 3 years. *Kidney Int.* **76**, 149-168 (2009).
2. Chapman, A. B., *et al.* Kidney volume and functional outcomes in autosomal dominant polycystic kidney disease. *Clinical journal of the American Society of Nephrology : CJASN.* **7**, 479-486 (2012).
3. Torres, V. E., Harris, P. C. Polycystic kidney disease: genes, proteins, animal models, disease mechanisms and therapeutic opportunities. *J Intern Med.* **261**, 17-31 (2007).
4. Hateboer, N., *et al.* Comparison of phenotypes of polycystic kidney disease types 1 and 2 European PKD1-PKD2 Study Group. *Lancet.* **353**, 103-107 (1999).
5. Rossetti, S., *et al.* Association of mutation position in polycystic kidney disease 1 (PKD1) gene and development of a vascular phenotype. *Lancet.* **361**, 2196-2201 (2003).
6. Chapman, A. B., *et al.* Renal structure in early autosomal-dominant polycystic kidney disease (ADPKD): The Consortium for Radiologic Imaging Studies of Polycystic Kidney Disease (CRISP) cohort. *Kidney international.* **64**, 1035-1045 (2003).
7. Grantham, J. J., *et al.* Volume progression in polycystic kidney disease. *N Engl J Med.* **354**, 2122-2130 (2006).
8. Schrier, R. W., *et al.* Blood Pressure in Early Autosomal Dominant Polycystic Kidney Disease. *The New England journal of medicine.* (2014).
9. Torres, V. E., *et al.* Angiotensin Blockade in Late Autosomal Dominant Polycystic Kidney Disease. *The New England journal of medicine.* (2014).
10. Wilson, P. D. Mouse models of polycystic kidney disease. *Curr Top Dev Biol.* **84**, 311-350 (2008).
11. Happe, H., Peters, D. J. Translational research in ADPKD: lessons from animal models. *Nature reviews. Nephrology.* (2014).
12. Frahm, J., Haase, A., Matthaei, D. Rapid NMR imaging of dynamic processes using the FLASH technique. *Magnetic resonance in medicine : official journal of the Society of Magnetic Resonance in Medicine / Society of Magnetic Resonance in Medicine.* **3**, 321-327 (1986).
13. Bae, K. T., *et al.* Magnetic resonance imaging evaluation of hepatic cysts in early autosomal-dominant polycystic kidney disease: the Consortium for Radiologic Imaging Studies of Polycystic Kidney Disease cohort. *Clin J Am Soc Nephrol.* **1**, 64-69 (2006).
14. Hossack, K. F., Leddy, C. L., Johnson, A. M., Schrier, R. W., Gabow, P. A. Echocardiographic findings in autosomal dominant polycystic kidney disease. *N Engl J Med.* **319**, 907-912 (1988).
15. Lumiaho, A., *et al.* Mitral valve prolapse and mitral regurgitation are common in patients with polycystic kidney disease type 1. *American journal of kidney diseases : the official journal of the National Kidney Foundation.* **38**, 1208-1216 (2001).
16. Vallee, J. P., Ivancevic, M. K., Nguyen, D., Morel, D. R., Jaconi, M. Current status of cardiac MRI in small animals. *Magma.* **17**, 149-156 (2004).
17. Epstein, F. H. MR in mouse models of cardiac disease. *NMR Biomed.* **20**, 238-255 (2007).
18. Bloomgarden, D. C., *et al.* Global cardiac function using fast breath-hold MRI: validation of new acquisition and analysis techniques. *Magnetic resonance in medicine : official journal of the Society of Magnetic Resonance in Medicine / Society of Magnetic Resonance in Medicine.* **37**, 683-692 (1997).
19. Larson, A. C., *et al.* Self-gated cardiac cine MRI. *Magnetic resonance in medicine : official journal of the Society of Magnetic Resonance in Medicine / Society of Magnetic Resonance in Medicine.* **51**, 93-102 (2004).
20. Smith, J. C., Corbin, T. J., McCabe, J. G., Bolon, B. Isoflurane with morphine is a suitable anaesthetic regimen for embryo transfer in the production of transgenic rats. *Laboratory animals.* **38**, 38-43 (2004).
21. Ahrens, E. T., Srinivas, M., Capuano, S., Simhan, H. N., Schatten, G. P. Magnetic resonance imaging of embryonic and fetal development in model systems. *Methods Mol Med.* **124**, 87-101 (2006).
22. Zhou, R., Pickup, S., Glickson, J. D., Scott, C. H., Ferrari, V. A. Assessment of global and regional myocardial function in the mouse using cine and tagged MRI. *Magnetic resonance in medicine : official journal of the Society of Magnetic Resonance in Medicine / Society of Magnetic Resonance in Medicine.* **49**, 760-764 (2003).
23. Stimpfel, T. M., Gershey, E. L. Selecting anesthetic agents for human safety and animal recovery surgery. *FASEB journal : official publication of the Federation of American Societies for Experimental Biology.* **5**, 2099-2104 (1991).